JCTC Journal of Chemical Theory and Computation

ARTICLE

pubs.acs.org/JCTC

Nonorthogonality Problem and Effective Electronic Coupling Calculation: Application to Charge Transfer in π-Stacks Relevant to Biochemistry and Molecular Electronics

Agostino Migliore*,†

†School of Chemistry, Tel Aviv University, Tel Aviv 69978, Israel

Supporting Information

ABSTRACT: A recently proposed method for the calculation of the effective electronic coupling (or charge-transfer integral) in a two-state system is discussed and related to other methods in the literature. The theoretical expression of the coupling is exact within the two-state model and applies to the general case where the charge transfer (CT) process involves nonorthogonal initial and final diabatic (localized) states. In this work, it is shown how this effective electronic coupling is also the one to be used in a suitable extension of Rabi's formula to the nonorthogonal representation of two-state dynamical problems. The formula for the transfer integral is inspected in the regime of long-range CT and applied to CT reactions in redox molecular systems of interest to biochemistry and/or to molecular electronics: the guanine−thymine stack from regular B-DNA, the polyaromatic perylenediimide stack, and the quinol-semiquinone couple. The calculations are performed within the framework of the Density Functional Theory (DFT), using hybrid exchange-correlation (XC) density functionals, which also allowed investigation of the appropriateness of such hybrid-DFT methods for computing electronic couplings. The use of the recently developed M06-2X and M06-HF density functionals in appropriate ways is supported by the results of this work.

1. INTRODUCTION

The recent progress in molecular electronics fostered a considerable increase in experimental,[1−7] and theoretical,[2,3,8−14] investigations of CT in molecular systems. From a theoretical point of view, many efforts have been devoted to the understanding and quantification of the CT efficiency in molecular systems, which depends crucially on the reorganization energy (that is, the free energy change caused by the nuclear rearrangement that follows a CT process) and the charge-transfer integral between the hole or electron donor and acceptor groups.[11,15] This is particularly evident within the framework of Marcus electron transfer theory,[16,17] where the transfer rate constant is expressed as[18]

$$k_{ET} = \kappa(V_{IF})\nu \exp\left[-\frac{(\Delta G^0 + \lambda)^2}{4\lambda k_B T}\right] \quad (1)$$

In eq 1, κ is the electronic transmission coefficient, which depends on the effective electronic coupling V_{IF} and is proportional to the mean-square value of V_{IF} in the nonadiabatic limit (i.e., for suitably weak coupling between the charge donor and acceptor species[19]). ν is an effective frequency that characterizes the nuclear motion along the reaction coordinate, λ is the reorganization energy, ΔG^0 is the reaction free energy, k_B is Boltzmann's constant, and T is the temperature. λ is the only relevant parameter in the exponential nuclear factor for self-exchange reactions, where ΔG^0 is zero. Depending on the system, eq 1 yields, indeed, the rate constant for electron or hole transfer reactions, the latter being described, in all respects considered in this paper, as electron transitions in the reverse direction of the hole transfer in a system with a net positive charge.

The rate in eq 1 is an important quantity not only for CT reactions between redox molecular centers but also in molecular electronics, where it is strictly related to the electrical conductance through metal−molecule−metal junctions, especially in the regime of weak molecule−metal couplings,[9,18,20] from whence comes the importance of accurate calculations of the involved physical parameters. As shown by eq 1, V_{IF} can play a crucial role in determining the value of k_{ET} and also provides a compact link between k_{ET} and the electronic properties of the system.

Disparate approaches to accurate calculation of transfer integrals have been used in the literature,[8,21−34] with an increasing presence of DFT or hybrid-DFT approaches.[14,33−37] This trend relies on (i) the fact that DFT computational schemes include electron correlation and can be applied to larger systems than those allowed by reliable *ab initio* approaches other than Hartree−Fock (HF). On the other hand, the HF approach does not include the so-called correlation energy. Thus, DFT offers the best compromise between accuracy and feasibility for the study of most (bio)molecular systems of relevance to nanoelectronics.[38] The trend also relies on (ii) the elaboration of new hybrid XC functionals, with continuous improvement in their ability to correct for the presence of unphysical electron self-interaction. Indeed, hybrid functionals mostly perform better than self-interaction corrected DFT schemes.[39] Moreover, correcting their residual self-interaction errors does not necessarily improve their description of molecular properties.[39]

Most quantum chemical methods for the computation of transfer integrals need to cope with a suitable definition of the

Received: March 21, 2011
Published: April 26, 2011

involved diabatic states that describe the different localization of the transferring charge before and after the hole or electron transition. Ref 34 provides an expression of the effective electronic coupling, which is exact within the two-state model and does not make any assumption about the overlap between the diabatic electronic states. Such formulation is in harmony with the fact that in most physical situations[15] the localization of the (transferring) excess charge in different redox sites leads to electronic distributions with nonzero spatial overlap. Thereby, its application can help physical interpretation (see, e.g., section 2.4) and lead to practical advantages. On the other hand, the same V_{IF} value is obtained by using diabatic states with different overlaps (or orthogonal ones), as long as the two-state approximation is satisfied, a sufficiently accurate computational level is used, and the different diabatic representations are suitably related, as discussed in the next section.

The method in ref 34 is a generalization of that in ref 33. The relation between both approaches and previous literature[15,40−42] is discussed in sections 2.1 and 2.2. It is worth mentioning, in this regard, that ref 43 calculates, within a two-electron valence bond model, and compares coupling matrix elements between the electronic states of diatomic systems in different representations (the adiabatic representation, a nonorthogonal diabatic representation, and a symmetrically orthogonalized diabatic representation). The role of V_{IF} in the transition probability at fixed nuclear coordinates is investigated in section 2.3. Sections 2.2 and 2.3 provide a full analytical basis for the correct form of the "effective" coupling or perturbation to be used in nonorthogonal representations of the two-state dynamics. The investigation of the long-range behavior of V_{IF} in section 2.4 contributes to an exhaustive analysis of the role played by the overlap between the diabatic states in determining the effective electronic coupling. Then, the systems under consideration and the used computational setups are described in section 3. Applications follow in section 4. The V_{IF} calculations provided in this work highlight limitations, advantages, and suitable uses of the considered hybrid-DFT implementations. The comparison with previous results in the literature using Hartree−Fock (HF), multireference,[44] DFT,[14,30] and other constrained DFT[37] approaches contributes to restricting the ranges of expectation values of V_{IF} in the studied systems, in view of future experimental validation and applications.

2. THEORY

2.1. Effective Electronic Coupling Calculations Using Diabatic States with Zero and Nonzero Overlap. Within the two-state model, the ground-state vector of a system is written as

$$|\psi\rangle = a|\psi_I\rangle + b|\psi_F\rangle = a_0|\chi_I\rangle + b_0|\chi_F\rangle \quad (2)$$

where the nonorthogonal wave functions ψ_I and ψ_F, or the orthogonal ones χ_I and χ_F, represent the reactant and product states, respectively, as introduced in the diabatic picture of charge transfer. In these diabatic states, the excess charge is localized on the donor and acceptor, respectively, at any value of the chosen reaction coordinate Q[45] (see Figure 1). The energy profile shows a splitting between the adiabatic ground and first excited states at the transition state coordinate (here called Q_t), where the diabatic states are degenerate. At such a coordinate, both the requirement of energy conservation and the Franck−Condon principle[46] are satisfied in the transition from a diabatic state to the other, and the corresponding Franck−Condon factor takes its maximum.

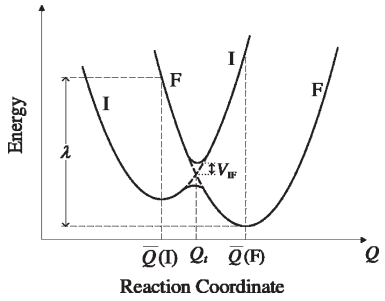

Figure 1. Cross-section of the (free) energy profile for the initial (I) and final (F) electronic states of a typical electron transfer reaction. The solid and dashed curves describe the adiabatic and diabatic states, respectively. $\overline{Q}(I)$ and $\overline{Q}(F)$ are the equilibrium coordinates of states I and F, respectively. Q_t is the transition state coordinate, which corresponds to the lowest energy on the crossing seam surface. The reorganization energy λ is also shown.

The separation ΔE_v of the adiabatic energies at Q_t gives a measure of the effective electronic coupling V_{IF} between $|\psi_I\rangle$ and $|\psi_F\rangle$. This splitting can be easily obtained from the secular equation

$$\begin{vmatrix} H_{II} - \varepsilon & H_{IF} - \varepsilon S_{IF} \\ H_{IF} - \varepsilon S_{IF} & H_{FF} - \varepsilon \end{vmatrix} = 0 \quad (3)$$

where H is the Hamiltonian of the two-state system, ε is the energy eigenvalue, $H_{II} = \langle\psi_I|H|\psi_I\rangle$ and $H_{FF} = \langle\psi_F|H|\psi_F\rangle$ are the energies of the diabatic states, $H_{IF} = \langle\psi_I|H|\psi_F\rangle$ is their electronic coupling, and $S_{IF} = \langle\psi_I|\psi_F\rangle$ is their overlap. The eigenvalues of eq 3 can be written in the implicit form[47]

$$E_\pm = \frac{1}{2}[H_{II} + H_{FF} \pm \sqrt{\Delta E_{IF}^2 + 4(H_{IF} - E_\pm S_{IF})^2}] \quad (4)$$

where $\Delta E_{IF} = E_I - E_F \equiv H_{II} - H_{FF}$ is the energy difference, at the given nuclear configuration, between the CT initial (I) and final (F) diabatic states. Then, the vertical excitation energy can be written as[34,48]

$$\Delta E_v \equiv E_+ - E_- = \sqrt{\frac{\Delta E_{IF}^2}{1 - S_{IF}^2} + 4V_{IF}^2} \quad (5)$$

(so that $\Delta E_v = 2V_{IF}$ at $Q = Q_t$, where $E_I = E_F$[49]), where

$$V_{IF}(Q) \equiv \frac{1}{1 - S_{IF}^2(Q)}\left|H_{IF}(Q) - S_{IF}(Q)\frac{H_{II}(Q) + H_{FF}(Q)}{2}\right| \quad (6)$$

is the CT matrix element or effective electronic coupling or transfer integral.[8] According to the Condon approximation,[18] the dependence of V_{IF} on the nuclear degrees of freedom, which is explicitly shown in eq 6, is neglected all along the Q axis. When such approximation is not fulfilled, a meaningful value of $V_{IF}(Q)$ to be inserted into eq 1 for calculating the CT rate needs to be obtained close enough to Q_t, i.e., in the proximity of the crossing seam point of Figure 1. The possible dependence on Q is not explicitly shown in the next equations. If orthogonal diabatic states are used (e.g., the localized states are obtained by suitable rotation of the adiabatic states), then $V_{IF} = H_{IF}$, and the effective electronic coupling can be written in terms of a_0 and b_0 as

$$V_{IF} = H_{IF} = a_0 b_0 \Delta E_v \quad (7)$$

This formula appears in ref 41, besides another original approach that makes use of the quasi-degenerate perturbation theory and where the determination of the adiabatic energies or diabatic wave functions is not compulsory, as only electron correlation contributions to H_{IF} are explicitly computed.

By using eq 5 for zero S_{IF} and relating a_0 and b_0 to the adiabatic and diabatic dipole moments, under the assumption of weakly interacting diabatic states connected by a zero transition dipole moment (thus, first order perturbation theory can be used), eq 7 becomes[22,42,50,51]

$$V_{IF} = \frac{|\mu_{-+}|\Delta E_{IF}}{|\Delta\mu_{IF}|} \tag{8}$$

where μ_{-+} is the transition dipole moment that connects the adiabatic states and $\Delta\mu_{IF}$ is the difference between the dipole moments of the diabatic states. Equation 8 represents the Mulliken−Hush approach to the calculation of $V_{IF} = H_{IF}$. As shown in refs 42 and 50d, eq 8 may be extended to the nonperturbative regime by replacing ΔE_{IF} with ΔE_v. In ref 22a, the generalized Mulliken-Hush (GMH) model is introduced, which (i) retains the assumption that the diabatic states localized at different sites have zero off-diagonal dipole moment matrix elements, (ii) is not restricted to a perturbative treatment within the state space of interest, and (iii) does not require approximation of $\Delta\mu_{IF}$ using structural data. In a two-state system, by expressing $\Delta\mu_{IF}$ in terms of the adiabatic dipole moments μ_- and μ_+, and their difference $\Delta\mu_{-+}$, the following result is obtained[22]

$$V_{IF} = \frac{\Delta E_v|\mu_{-+}|}{\sqrt{(\Delta\mu_{-+})^2 + 4\mu_{-+}^2}} \tag{9}$$

where also eq 5 written for zero overlap is exploited.

Contrary to the GMH method, in ref 33, the transfer integral V_{IF} is expressed exclusively in terms of quantities that pertain to diabatic states with generally nonzero overlap, as

$$V_{IF} = \left|\frac{ab}{a^2 - b^2}\Delta E_{IF}\right| \tag{10}$$

This also avoids calculation of the vertical excitation energy, with evident advantages for the application of eq 10 in DFT schemes, e.g., for the *ab initio* study of large portions of biochemical systems. Moreover, it provides a useful link, for $Q \rightarrow Q_t$ (where eq 10 has an eliminable discontinuity), with the concept of resonance energy widely used in valence bond theory (cf. eqs 8 and 11 in ref 34 with eq 10 in ref 52). In ref 33, eq 10 was derived from the secular equation, eq 3, in the presence of a suitably small overlap. In ref 34, it is shown that, irrespective of the values of S_{IF} and Q, V_{IF} is exactly given by (wave function overlap method)

$$V_{IF} = \left|\frac{ab}{a^2 - b^2}\Delta E_{IF}\left(1 + \frac{a^2 + b^2}{2ab}S_{IF}\right)\frac{1}{1 - S_{IF}^2}\right| \tag{11a}$$

or, equivalently,

$$V_{IF} = \left|\frac{AB}{A^2 - B^2}\Delta E_{IF}\left(1 - \frac{A^2 + B^2}{2AB}S_{IF}\right)\frac{1}{1 - S_{IF}^2}\right| \tag{11b}$$

where the overlap integrals $A \equiv \langle\psi_I|\psi\rangle = a+bS_{IF}$ and $A \equiv \langle\psi_F|\psi\rangle = b+aS_{IF}$ have been inserted. In the same work, it is shown that eq 10 can indeed be used as an approximation of eqs 11, at any coordinate Q and in terms of either a and b or A and B, if S_{IF} is much smaller than $2ab$ or $2AB$. Such a a condition is much weaker than neglecting S_{IF}. In fact, it allows S_{IF} values that can lead to a considerable difference between the effective electronic coupling V_{IF} and the electronic coupling H_{IF},[18,30,36,53] related as in eq 6. For $S_{IF} \ll 2ab$, the insertion of eq 11 into eq 5 and the Taylor expansion of eq 5 up to the zero-order term in $S_{IF}/(2ab)$ gives

$$\Delta E_v = \left|\frac{a^2 + b^2}{a^2 - b^2}\Delta E_{IF}\right| \tag{12}$$

By combining eqs 10 and 12, it is seen that the right-most term of eq 7 still provides a formal expression for V_{IF} after replacement of a_0 and b_0 with a and b, respectively, while $V_{IF} \neq H_{IF}$. In other words, whereas for zero overlap eqs 7 and 10 are equivalent solutions of the secular equation and essentially differ by the respectively required computational approaches, for $S_{IF}/(2ab) = o(1) \neq 0$ (as it is in several cases[11,30,34,48,53−56]), the use of nonorthonal diabatic states for the direct (i.e., without prior and suitable orthogonalization) computation of V_{IF} is allowed only by eq 10 or, within the limits of applicability of eq 12, by a modified eq 7 where the overlap-dependent coefficients

$$a = \frac{A - BS_{IF}}{1 - S_{IF}^2},\ b = \frac{B - AS_{IF}}{1 - S_{IF}^2} \tag{13}$$

are employed. In many other cases,[8,15,34,40,57−59] the diabatic states that rely on physically meaningful approximations (e.g., the valence bond structures that correspond to the reactants and products of the CT reaction[15,59]) have an overlap that is not negligible compared to $2ab$ or is even larger than this quantity. For example, the value of S_{IF} can be an appreciable fraction of unity in short-range CT reactions, or, for weakly coupled redox sites, the valence charge in the ground state can be mostly localized around one of them, so that a or b is almost unity and the other coefficient is much less than unity. In all such cases, the modified eq 7 and eq 10 are not equivalent approximations to the exact analytical solution of the secular equation provided by eq 11, and both fail in quantifying the transfer integral from nonorthogonal states, for which eq 11 can be used. Ultimately, eqs 9 and 11 represent alternative theoretical approaches to the calculation of effective electronic couplings in the adiabatic and diabatic representations, respectively.

2.2. Wave Function Overlap Method and Diabatic States. As discussed in the previous literature,[15,40,59,60] the definition of effective diabatic states is not unique. Thus, the use of a given set of diabatic states to describe the CT reaction under investigation generally needs to rely on physical grounds. This point was, e.g., considered in refs 34 and 48, where different sets of diabatic states were selected, on the basis of the structure of the system and the localization of the charge in the donor and acceptor centers, in order to describe hole transfer through DNA nucleobase stacks. Often, the I and F diabatic electronic states are constructed as the valence bond structures of the involved reactants and products.[15,59] For instance, ref 59 provides an interesting model for deriving effective diabatic states using *ab initio* self-consistent field bond theory. An interesting and fruitful DFT approach to charge localization is provided by constrained DFT (CDFT),[32] where the addition of a suitable external effective potential to the Hamiltonian of the CT system allows one to obtain self-consistently the lowest-energy I and F states, under the approximations of the given XC functional and the basis set used to expand the electron wave functions. The uncertainty

in the definition of the CDFT diabatic states in general decreases with the separation of the charge donor and acceptor groups.[32] Nevertheless, eq 11 suggests the possibility of using CDFT diabatic states also in various short-range (and intramolecular) CT processes. The appropriateness of the CDFT approach to charge localization in such contexts is mainly the subject of future work. In this paper, the investigation of this point is limited to (i) a guanine−thymine base stack from regular DNA, which is characterized by the largest intrastrand effective electronic coupling among the DNA nucleobase stacks and a related large overlap integral between CDFT-type diabatic states,[34] and (ii) the quinol−semiquinone redox couple, on the short-distance side of Figure 4.

In this paper, the use of eq 11 with CDFT diabatic states, and a suitable choice of basis set and hybrid XC density functional, is proposed as an efficient hybrid-DFT theoretical-computational method for the first-principles calculation of the effective electronic coupling in various molecular systems of interest to biochemistry and nanoelectronics. Also, other valuable methods for the construction of diabatic states[15,30,53,61] can be combined indeed with the use of eq 11. Such implementations can be fruitful and are desirable, but they are out of the scope of the present work. On the other hand, tensor product (TP) diabatic states are also employed in section 4.1. In general, such states can be used for separated redox sites and in very accurate computational schemes (see, e.g., Table 1, where the largest Pople-style basis set is used).[34,48]

The consistency of using sets of diabatic states characterized by different overlaps can be investigated and rationalized by exploiting the Löwdin transformation.[40,43] In particular, it is important to understand to what extent orthogonal and nonorthogonal diabatic representations can be consistently adopted in order to calculate the charge-transfer integral for a given redox system. To this aim, consider first the general case where physically meaningful assumptions (e.g., based on the involved valence bond structures) lead to diabatic wave functions ψ_I and ψ_F[62] with appreciable overlap S_{IF} that provide a good description of the CT reaction under investigation, as validated by comparison with relevant experimental data. I will call $\mathbf{\Psi} = (\psi_I\ \psi_F)$ the reference diabatic set. An equivalent orthonormal diabatic set is obtained using the Löwdin transformation[40]

$$\boldsymbol{\chi} = \mathbf{\Psi}\mathbf{S}^{-1/2} \tag{14}$$

where $\boldsymbol{\chi} = (\chi_I\ \chi_F)$ and $\mathbf{S}$ is the overlap matrix defined as

$$\mathbf{S} = \begin{pmatrix} 1 & S_{IF} \\ S_{IF} & 1 \end{pmatrix} \tag{15}$$

The insertion of $\boldsymbol{\chi}$ in eq 7 or eq 10 with $a = a_0$ and $b = b_0$ leads to the same V_{IF} value that results from the application of eq 11 in the $\mathbf{\Psi}$ representation. In fact, as shown by eq 48 (see Appendix), insertion of eq 14 into eq 10 leads to eq 11. Considering that $\boldsymbol{\chi}$ can also be obtained by rotation of the adiabatic states,[27] eq 14 fixes the rotation angle that relates the suitable diabatic representation to the adiabatic one in any direct use of eq 7 by exploiting orthogonal diabats. On the other hand, eq 11 provides a general expression of the effective electronic coupling in terms of a few electronic quantities that characterize the orthogonal diabatic representation (in this case, the overlap in the expression of V_{IF} is zero) or any nonorthogonal diabatic representation, which is related to $\boldsymbol{\chi}$ by the Löwdin orthogonalization in eq 14 and to the reference representation by the equation (see Appendix)

$$\overline{\mathbf{\Psi}} = \mathbf{\Psi}\mathbf{M} \tag{16}$$

where $\mathbf{M}$ is the symmetric matrix

$$\mathbf{M} = \frac{1}{2}\begin{pmatrix} \sqrt{(1+\overline{S}_{IF})/(1+S_{IF})} + \sqrt{(1-\overline{S}_{IF})/(1-S_{IF})} & \sqrt{(1+\overline{S}_{IF})/(1+S_{IF})} - \sqrt{(1-\overline{S}_{IF})/(1-S_{IF})} \\ \sqrt{(1+\overline{S}_{IF})/(1+S_{IF})} - \sqrt{(1-\overline{S}_{IF})/(1-S_{IF})} & \sqrt{(1+\overline{S}_{IF})/(1+S_{IF})} + \sqrt{(1-\overline{S}_{IF})/(1-S_{IF})} \end{pmatrix} \tag{17}$$

and $\overline{S}_{IF} = \langle\bar{\psi}_I|\bar{\psi}_F\rangle$. Equation 14 is clearly the special case of eq 16 for $\overline{S}_{IF} = 0$.

In many circumstances, different diabatic sets can provide convenient representations of the given CT system (e.g., this can be the case in section 4.1). Even if these diabatic representations are related as in eq 17, various sources of error can clearly lead to different values of the effective electronic coupling and/or the vertical excitation energy or to consistently wrong results. For example, DFT calculations are generally affected by the presence of spurious electron self-interaction,[63] although hybrid XC functionals can yield optimal correction, also depending on the system.[39] Then, since different sets of diabatic states correspond to diverse electron localizations, the corresponding energies may differently suffer from self-interaction, thus leading to different values of V_{IF} even if eq 17 is fulfilled and eq 11 is employed. On the contrary, but for analogous reasons, similar values can arise from diabatic sets which are not related as in eq 17. At any rate, eq 17 can generally provide a helpful check of the consistency and robustness of the computational results. Then, differences in the results can even become a source of useful information.

Finally, it is worth noting that the connection between eq 11 and the Löwdin transformation can be reformulated in terms of the Hamiltonian operator $\mathbf{H}$ of the CT system. In fact, the relation between the orthogonal and nonorthogonal diabatic sets is an expression of the fact that the algebraic problem of the secular equation including the S_{IF} terms is reduced to the zero overlap form if the matrix $\mathbf{H}$ is replaced by the self-adjoint matrix[40,64]

$$\mathbf{H}' = \mathbf{S}^{-1/2}\mathbf{H}\mathbf{S}^{-1/2} \tag{18}$$

The insertion of eq 41 from the Appendix into eq 18 and comparison with eq 6 yields

$$|H'_{IF}| = \left| H_{IF} - \frac{H_{II} + H_{FF}}{2}S_{IF} + H_{IF}S_{IF}^2 - + \ldots \right| = V_{IF} \tag{19}$$

which reduces to the usually adopted small-overlap Löwdin transformation,[30,40,53]

$$V_{IF} = H_{IF} - \frac{H_{II} + H_{FF}}{2}S_{IF} \tag{20}$$

when the terms nonlinear in S_{IF} can be disregarded. Alternatively, eq 19 is indeed formulated by eq 48 in the Appendix. In conclusion, (i) the exact expression of the effective electronic

coupling in terms of a few electronic quantities that characterize the diabatic states and their connection with the ground state was obtained in ref 34 by direct solution of the secular equation, using the definition (eq 6) of V_{IF}; (ii) it is[33,34,41,42]

$$V_{IF} = \begin{cases} \langle \chi_I | H_{IF} | \chi_F \rangle = |a_0 b_0 \Delta E_v| = \left| \frac{a_0 b_0}{a_0^2 - b_0^2} \Delta E_{IF}^0 \right| & S_{IF} = 0 \\ \langle \psi_I | H_{IF}' | \psi_F \rangle \cong \left| \frac{ab}{a^2 - b^2} \Delta E_{IF} \right| & S_{IF} = o(2ab) \le o(1) \\ \langle \psi_I | H_{IF}' | \psi_F \rangle = \left| \frac{ab}{a^2 - b^2} \Delta E_{IF} \left(1 + \frac{a^2 + b^2}{2ab} S_{IF} \right) \frac{1}{1 - S_{IF}^2} \right| & \forall\ S_{IF} \end{cases} \tag{21}$$

where ΔE_{IF}^0 is the diabatic energy difference between χ_I and χ_F; (iii) V_{IF} is invariant under the Löwdin transformation, hence, in general, under the change of representation defined by the **M** matrix in eq 17.

In ref 34, I stressed that the calculation of V_{IF} directly from eq 6 or 20 is generally very sensitive to the value of S_{IF}, especially if the involved matrix elements are computed in a multielectron scheme. In fact, in this case, the right-hand side of eq 6 involves a delicate numerical difference of two energy quantities much larger than their difference (see also p 28 of ref 18). Equation 11 allows one to avoid this critical point. On the other hand, both the numerator and the denominator of eq 11 tend to zero at the transition state coordinate Q_t. However, as is demonstrated in ref 34, the expression of V_{IF} in eq 11 (i) has an eliminable discontinuity at Q_t, (ii) has the correct behavior for $Q \to Q_t$, and (iii) allows calculation of V_{IF} with high accuracy even when Q is very close to Q_t, as quantified by the fact that $\Delta E_{IF}(Q) \ll 2V_{IF}(Q)$ and thus the relative difference between $2V_{IF}(Q)$ and $\Delta E_v(Q)$ is correspondingly small. Point iii was noticed in ref 48 and is strongly supported by the cogent computational test in section 4.2 of this work.

2.3. Electron Transition Probability at Fixed Nuclear Coordinates. As shown by eq 1, V_{IF} plays a crucial role in determining the electronic transmission coefficient κ that appears in the electron transfer rate. Near the transition state coordinate, the electron transitions that can be caused by this coupling are mixed with the nuclear dynamics, which, overall, leads to the expression of κ. While the interplay of the electron and nuclear dynamics has been treated in different, though related, ways in the literature,[16,17,19,65−67] common appreciation of those treatments is that the nuclear coordinates can be taken as external parameters at the short times when a single electron transfer event occurs. This leads to tackling the time-dependent Schrödinger equation for the electronic state of the system. The electron distributions before and after a CT event are clearly not eigenstates of the overall system and represent, in general,[18,66] nonorthogonal states. This is, e.g., explicitly considered in ref 66, where the ground-state wave function at a generic time t is expanded on two nonorthogonal wave functions

$$\psi(t) = C_I(t)\psi_I + C_F(t)\psi_F \tag{22}$$

with $\langle \psi_I | \psi_F \rangle = S_{IF}$, and the time-dependent Schrödinger equation

$$i\hbar \frac{\partial}{\partial t} [C_I(t)\psi_I + C_F(t)\psi_F] = H[C_I(t)\psi_I + C_F(t)\psi_F] \tag{23}$$

is solved under the initial conditions

$$C_I(0) = 1; C_F(0) = 0. \tag{24}$$

This led to an expression of $|C_F(t)|^2$ (used as an expression of the probability of electron transfer at the given nuclear coordinates) that extended Rabi's formula for this square coefficient to the nonorthogonal set of electronic states, and where the "effective" coupling or perturbation is not symmetric with respect to the two diabatic states. In fact, it appears in the form $H_{FI} - H_{II}S_{FI}$, which is different from that in eq 6 and is an off-diagonal element of the Hamiltonian matrix **H** in the $\mathbf{\Psi} = (\psi_I\ \psi_F)$ representation. **H** is non-Hermitian for $H_{II} \neq H_{FF}$[68] and is obtained by multiplying eq 23 by ψ_S^* (S = I, F; a standard notation for complex conjugate quantities is used) and integrating it over the spatial coordinates, which gives[66]

$$i\hbar \frac{\partial}{\partial t} \mathbf{C}(t) = \mathbf{H}\mathbf{C}(t) \tag{25a}$$

where **C** is the column vector of components C_I and C_F and[69]

$$\mathbf{H} = \frac{1}{1 - S_{IF}^2} \begin{pmatrix} H_{II} - H_{IF}S_{IF} & H_{IF} - H_{FF}S_{IF} \\ H_{IF} - H_{II}S_{IF} & H_{FF} - H_{IF}S_{IF} \end{pmatrix} \tag{25b}$$

Various devices were conceived to achieve the desired Hermitian behavior within a purely electronic framework.[15] In ref 18, it is argued that the off-diagonal terms of the **H** operator in eq 25b include two contributions: "part of the perturbation induces the transition while other parts distort the zero order states to be coupled".[18] Now, I decompose the Hamiltonian in eq 25b as follows:

$$\mathbf{H} = \begin{pmatrix} \frac{1}{1 - S_{IF}^2}(H_{II} - H_{IF}S_{IF}) & V_{IF} \\ V_{IF} & \frac{1}{1 - S_{IF}^2}(H_{FF} - H_{IF}S_{IF}) \end{pmatrix} + \frac{1}{1 - S_{IF}^2} \begin{pmatrix} 0 & \frac{\Delta E_{IF}}{2} S_{IF} \\ -\frac{\Delta E_{IF}}{2} S_{IF} & 0 \end{pmatrix} \tag{26}$$

where V_{IF} and ΔE_{IF} are defined as above. The first matrix is Hermitian, and its off-diagonal element V_{IF} is the effective electronic coupling that determines, essentially, the probability of transition. To see this, it is necessary to recognize that, since ψ_I and ψ_F, though nonorthogonal, are the initial and final states, the probabilities of interest are given by $|\langle \psi_{I,F} | \psi(t) \rangle|^2$. According to eq 24, the system is initially in state $|\psi_I\rangle$, which does not entail zero probability of finding the system in state $|\psi_F\rangle$, because of the nonzero overlap between the two electronic states. In fact, $|\langle \psi_F | \psi(0) \rangle|^2 = S_{IF}^2$. Note that this probability is well-defined irrespective of the partner wave function chosen to expand $\psi(0)$. In fact, it results also from the decomposition of $\psi(0)$ in ψ_F and the wave function orthogonal to ψ_F, i.e., $\psi(0) = S_{IF}\psi_F + (1 - S_{IF}^2)^{1/2}\bar{\psi}_I$ with $\bar{\psi}_I = (\psi_I - S_{IF}\psi_F)/(1 - S_{IF}^2)^{1/2}$. Then, one is interested in the probability that the system is in state ψ_F at a later time t, that is, $|\langle \psi_F | \psi(t) \rangle|^2$. The fact that $S_{IF} \neq 0$ means, simply, that the probability of finding the system in ψ_I at time t, given by $|\langle \psi_I | \psi(t) \rangle|^2$, is not equal to $1 - |\langle \psi_F | \psi(t) \rangle|^2$. In order to calculate the transition probability $|\langle \psi_F | \psi(t) \rangle|^2$, first I consider that eq 22 and the normalization condition on ψ give

$$|\langle \psi_F | \psi(t) \rangle|^2 = 1 - (1 - S_{IF}^2)|C_I(t)|^2 \tag{27}$$

Insertion of eq 26 into eq 25a and application of the Laplace transform method yields

$$C_1(t) = \frac{1}{2}\left[(e^{u_+t} + e^{u_-t}) - \frac{1}{1 - S_{IF}^2}\frac{\Delta E_{IF}}{\Delta E_v}(e^{u_+t} - e^{u_-t})\right] \quad (28a)$$

where ΔE_v is given by eq 5 and

$$u_\pm = -\frac{i}{\hbar}\left[\frac{1}{1 - S_{IF}^2}\left(\frac{H_{II} + H_{FF}}{2} - S_{IF}H_{IF}\right) \mp \frac{\Delta E_v}{2}\right] \quad (28b)$$

Finally, insertion of eqs 28 into eq 27 gives

$$|\langle\psi_F|\psi(t)\rangle|^2 = S_{IF}^2\cos^2\left(\frac{\Delta E_v}{2\hbar}t\right) + \frac{4V_{IF}^2}{(\Delta E_v)^2}\sin^2\left(\frac{\Delta E_v}{2\hbar}t\right)$$
$$= S_{IF}^2 + \left[\frac{4V_{IF}^2}{(\Delta E_v)^2} - S_{IF}^2\right]\sin^2\left(\frac{\Delta E_v}{2\hbar}t\right) \quad (29)$$

The probability oscillates between ${S_{IF}}^2$ and $4{V_{IF}}^2/(\Delta E_v)^2$. As expected, also in the presence of S_{IF}, unity is attained only if $H_{II} = H_{FF}$. Equation 29 shows that V_{IF}, which is defined as in eq 6 and is the off-diagonal element of the Hermitian component of the **H** operator in eq 26, is the effective coupling that appears in the probability of transition between nonorthogonal states, which is an electron transition probability when ψ_I and ψ_F are the diabatic (or localized) states of a typical CT reaction. Notice that, although the decomposition in eq 26 is not necessary for the solution of eq 25a, it turned out to be useful to obtain the transition probability directly in terms of V_{IF} and ΔE_v and thereby to identify the effective perturbation that plays a crucial role in the amplitude of oscillation of eq 29.

Indeed, because of the overlap between ψ_I and ψ_F, there is a nonzero transition probability also for $V_{IF} = 0$. In this case, eq 29 becomes

$$|\langle\psi_F|\psi(t)\rangle|^2 = S_{IF}^2\cos^2\left(\frac{\Delta E_{IF}}{2\hbar\sqrt{1 - S_{IF}^2}}t\right) \quad (30)$$

so that the transition probability oscillates between zero and a maximum of ${S_{IF}}^2$. Such values correspond to $\psi = \bar{\psi}_I = (\psi_I - S_{IF}\psi_F)/(1 - {S_{IF}}^2)^{1/2}$, that is, the state orthogonal to ψ_F, and $\psi = \psi_I$. In fact, ψ_I is not an eigenstate of the Hamiltonian; thus the system evolves from it and, given the zero effective electronic coupling between ψ_I and ψ_F, the amplitude of the transition probability cannot overcome the initial value of S_{IF}, while it can reach zero. To understand it analytically, it is necessary to consider also the coefficient $C_2(t)$, which is provided in ref 66. By rearranging it in terms of V_{IF}, ΔE_{IF}, and ΔE_v (or, equivalently, proceeding as above), and choosing a phase factor consistent with the choice in eqs 28, the following is written:

$$C_2(t) = -\frac{H_{IF} - H_{II}S}{(1 - S_{IF}^2)\Delta E_v}(e^{u_+t} - e^{u_-t}) \quad (31)$$

By evaluating eqs 28 and 31 for $V_{IF} = 0$ and inserting them into eq 22, the following is obtained:

$$\psi = \cos\left(\frac{\Delta E_{IF}}{2\hbar\sqrt{1 - S_{IF}^2}}t\right)\psi_I - i\sin\left(\frac{\Delta E_{IF}}{2\hbar\sqrt{1 - S_{IF}^2}}t\right)\bar{\psi}_I \quad (32)$$

that is, an oscillation between ψ_I and $\bar{\psi}_I$ in a wave function subspace where the maximum overlap of ψ with ψ_F is given by S_{IF}, as stated above. A nonzero effective electronic coupling between ψ_I and ψ_F allows the system to go out of this subspace, which can be defined as a space "quasi-orthogonal" to ψ_F for small S_{IF} values. Then, the maximum transition probability is given by $4{V_{IF}}^2/(\Delta E_v)^2$, which has the same formal expression as in Rabi's formula but with new definitions for the involved quantities as in eqs 5 and 6. In conclusion, the above equations fully characterizes V_{IF} with the symmetric expression in eq 6 as the "effective" electronic coupling in the **Ψ** representation, without the use of any *ad hoc* device.

2.4. Overlap between the Diabatic States and Effective Electronic Coupling in Long-Range CT. The relation between effective electronic coupling and diabatic state overlap approximately reduces to a linear one in diverse circumstances:[70,71]

$$V_{IF} = CS_{IF} \quad (33)$$

where C is a suitable constant for the system under consideration. Relations of this form have been used to calculate the interatomic resonance integral[70] and also the effective electronic coupling at larger interatomic distances.[71] For CT between off-resonance states (as is the case, e.g., in DNA base stacks[11]), the long-range behavior of V_{IF} can be easily obtained without using empirical parameters, which can have useful implications for the study of many biochemical processes. If the given donor and acceptor centers are far enough, V_{IF} (as well as S_{IF}) is very small and the electron is almost completely localized on one redox site, e.g., $\psi = \psi_I$. Then, $a \cong 1$, and the normalization constraint $\langle\psi|\psi\rangle = a^2 + b^2 + 2Re(ab^*)S_{IF}$ yields $b = 0$, which would give zero effective coupling, or $b \cong -2sgn(a)S_{IF}$. Moreover, at a large enough distance, it is $V_{IF} \leq \Delta E_{IF} \cong \Delta E_v$, and the diabatic energy difference essentially arises from the distribution of the excess charge in different local environments, at the given internal coordinates of the two redox sites. This difference approaches the value $\Delta E_{IF}^{(0)}$ for infinitely separated redox sites. Thus, on the basis of the above considerations, eq 11 leads to

$$V_{IF} \cong \frac{3}{2}|\Delta E_{IF}|S_{IF} \cong \frac{3}{2}|\Delta E_v|S_{IF} \cong \frac{3}{2}|\Delta E_{IF}^{(0)}|S_{IF} \quad (34)$$

which fixes the constant C in eq 33 at the value $3/2|\Delta E_{IF}^{(0)}|$. The diabatic energy difference mainly determines the electron localization on one molecular site. If two diverse redox couples have the same value of $\Delta E_{IF}^{(0)}$ at suitable nuclear coordinates, different S_{IF} values indicate different effective electronic couplings, hence different abilities to spread the excess charge out of the occupied site. Before concluding this section, it is also worth noting the similarity between the expression (eq 34) of the transfer integral in terms of the vertical excitation energy, within the context of long-distance CT, and the relation between resonance energy and atomic orbital overlap in ref 70, where the resonance energy is written in a form similar to the off-diagonal elements in the **H** matrix of eq 25b and is set proportional to the ionization energy for the appropriate valence atomic orbital.

3. SYSTEMS AND COMPUTATIONAL METHODS

3.1. Systems and Purposes. The first system under investigation is a guanine−thymine (GT) stack from ideal B-DNA (Figure 2a). The hole transfer between G and T is reconsidered, after its study in ref 34 with the Becke-half an d-half[72] (BHH) hybrid XC functional, to test the performance of the recently developed M06-2X and M06-HF XC density functionals.[73−75] In fact, GT is the nucleobase stack with the largest intrastrand V_{IF}

and is a paradigmatic case of relevance to theoretical studies on CT through DNA strands. Moreover, since the influence of the sugar−phosphate backbone on the electronic coupling between the stacked nucleobases is negligible,[11] the backbone can be excluded from the first-principles calculation of V_{IF}. Thus, both the TP and CDFT diabatic states can be used to describe the through-space hole transfer between G and T.

The perylenediimide (PDI; Figure 2b) belongs to a class of polycyclic aromatic molecules that are promising materials for nanoelectronics (e.g., for organic photovoltaics and thin film transistors), due to their ability to organize in well-ordered π stacks and to support hole or electron transport.[14,76,77] Hence, the charge transfer integrals for hole and electron transfer through stacked PDI molecules are parameters of practical relevance. The calculations performed in this work pursue the following main objectives: (i) test the performance of the M06-2X and M06-HF functionals, once used in combination with eq 11, in this kind of extended aromatic system, where the high-nonlocality character of the functional can play an important role; (ii) verify the (high) accuracy of the proposed theoretical-computational approach also very near the transition state coordinate, where the Condon approximation can be safely assumed; (iii) contribute to identify, or restrict, the maximal range of reliable values for the involved hole and electron transfer integrals. In a similar fashion to previous works on DNA stacks,[48] this is done calculating the V_{IF} values at different levels of computational accuracy and comparing the results with valuable ones in the previous literature.[14]

The distance dependence of the transfer integral and the fulfillment of eq 34 are investigated on the electron transfer between a quinol and a semiquinone function in a face-to-face arrangement. Apart from the importance of the redox reactions involving this system in biology and medicine,[78,79] it was chosen as a paradigmatic case for testing the performance of the M06-HF density functional.

3.2. TP and CDFT Diabatic States. The DNA stack can be easily separated into a donor group $\mathscr{D}$ (i.e., one of the two nucleobases), where the hole is initially localized, and an acceptor group $\mathscr{A}$, receiving the transferring hole. Hence, the I and F electronic states can be conveniently defined as $|\psi_I\rangle = |\mathscr{D}^+\rangle|\mathscr{A}\rangle$ and $|\psi_F\rangle = |\mathscr{D}\rangle|\mathscr{A}^+\rangle$, respectively, where the charge localized on each base has been explicitly indicated. They are obtained as tensor products of reference states for the isolated $\mathscr{D}$ and $\mathscr{A}$ groups in the initial and final charge states. The necessary electronic wave functions are built as single Slater determinants of the lowest-lying occupied Kohn−Sham spin orbitals. The feasibility of this procedure also regarding the spin contamination problem[63] has been discussed in ref 33 (see also ref 80 and references therein). The A, B, and S_{IF} overlaps are obtained by exploiting the ET module in the NWChem computational chemistry package.[8,81] The ET module is not used otherwise. Afterward, the a and b coefficients are derived from eq 13. The energy difference between the TP diabatic states is obtained from

$$\Delta E_{IF} = (E_{D^+} + E_A) - (E_D + E_{A^+}) + W_{D^+-A} - W_{D-A^+} \quad (35)$$

$E_{\mathscr{D}^+}$, $E_{\mathscr{A}^+}$, $E_{\mathscr{D}}$, and $E_{\mathscr{A}}$ are the ground-state energies of the isolated subsystems in the indicated charge states, which are directly provided by self-consistent field DFT calculations on such subsystems. $W_{\mathscr{D}^+-\mathscr{A}}$ and $W_{\mathscr{D}-\mathscr{A}^+}$ are the interaction energies between $\mathscr{D}$ and $\mathscr{A}$ in states $|\psi_I\rangle$ and $|\psi_F\rangle$, respectively, which are computed as energies of electrostatic interaction by using restraint electrostatic potential (RESP) charges that fit the quantum mechanical electrostatic potential on a specified grid. This is performed through the ESP module in the NWChem program,[81] with hyperbolic restraining on the partial atomic charges. After suitable testing, the maximum distance between a grid point and any of the atomic centers was set at the value 0.5 nm, and a grid spacing of 0.008 nm was used.

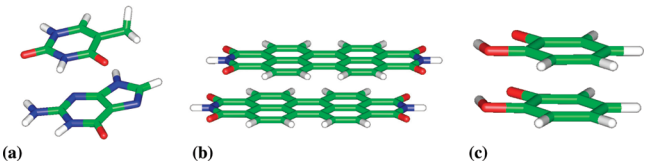

Figure 2. Molecular systems under consideration: (a) guanine-thymine (GT) stack from ideal B-DNA, (b) perylenediimide (PDI) stack, and (c) quinol−semiquinone redox couple.

Alternatively (and exclusively for the other two systems), the diabatic electronic states $|\psi_I\rangle$ and $|\psi_F\rangle$ are obtained from CDFT[32] calculations on the overall system, performed using NWChem. The CDFT approach consists of finding an effective external potential to add to the Hamiltonian in order to get the electronic state of lowest energy under the specified density constraint.[32] In hole (electron) transfer processes, a unit positive (negative) charge is localized in $\mathscr{D}$ ($\mathscr{A}$) for the initial (final) state. ΔE_{IF} is directly given by the difference between the energies E_I and E_F of the CDFT states. Hence, the approximations inherent in the partition scheme of eq 35 and consequent evaluation of $W_{\mathscr{D}^+-\mathscr{A}}$ and $W_{\mathscr{D}-\mathscr{A}^+}$ are avoided. The Löwdin population scheme was used in all of the CDFT calculations, whereas the Becke scheme turned out not to be feasible for the considered systems and hybrid-DFT approaches.

4. COMPUTATIONAL RESULTS AND DISCUSSION

4.1. Effective Electronic Coupling in the Guanine−Thymine Dimer. The charge-transfer and spatial overlap integrals for the GT nucleobase stack calculated in this work are reported in Table 1 (top panel). They are compared with previous results in the literature (bottom panel) based on the same set of atomic coordinates.[44]

Table 1 shows that the hole transfer integrals obtained by using the M06-2X functional are consistently overestimated (~40%) compared to those calculated in ref 34 with the BHH functional and the values from refs 30 and 44 which use the DFT fragment-orbital (FO) method and the GMH method combined with Koopmans' theorem[82] approximation (KTA),[26] respectively. Thus, on the basis of these results, the M06-2X functional should not be used for quantitative calculations of effective electronic couplings in DNA systems involving the GT stack.

On the contrary, the M06-HF functional, which uses full HF exchange, gives results that (i) are almost insensitive to the employed basis set and (ii) are in excellent agreement with the value of V_{IF} obtained in ref 44 by means of the second-order perturbation formulation (CAS-PT2) of the complete active space self-consistent field (CASSCF) method. In the reported multireference calculations, the full active space is indeed reduced to include 11 electrons in 12 π orbitals. Moreover, dynamic correlation is not included in the CASSCF approach. However, the CAS-PT2 calculations include the multistate formulation,

Table 1. (Upper Panel) Diabatic Energy Difference (ΔE_{IF}), Effective Electronic Coupling (V_{IF}) from eq 11, Overlap Integral (S_{IF}), and Vertical Excitation Energy (ΔE_v) from eq 5 for the 5′-GT-3′ Nucleobase Stack from Regular B-DNA, Calculated in This Work Using Both CDFT and TP Diabatic Electronic States[a] (Bottom Panel) Results from Hybrid-DFT,[34] DFT (with eq 20),[30] HF and Multireference[44] Calculations[b]

XC functional	basis set	ΔE_{IF}	V_{IF}	S_{IF}	ΔE_v	$\Delta E_{IF}^{(TP)}$	$V_{IF}^{(TP)}$	$S_{IF}^{(TP)} \equiv \bar{S}_{IF}$
				This Work				
M06-2x	6-31 g*	1.210	0.197	0.0629	1.274			
	6-311 g**	1.230	0.179	0.0761	1.284			
	cc-pVTZ	1.230	0.169	0.0826	1.280	1.248	0.1701	0.0171
	cc-pVTZ−BSSE					1.248	0.1701	0.0171
	6-311++g(3df,3pd)					1.217	0.168	0.0183
M06-HF	6-31 g*	1.207	0.078	0.0514	1.218			
	6-311 g**	1.232	0.077	0.0600	1.244			
	cc-pVTZ	1.258	0.078	0.0630	1.270	1.278	0.0804	0.0177
	cc-pVTZ−BSSE					1.281	0.0806	0.0177
	6-311++g(3df,3pd)					1.222	0.075	0.0195
				Ref 34				
BHH	6-31 g*	1.271	0.135	0.053	1.300	1.305	0.140	0.012
	6-311 g**	1.290	0.128	0.064	1.317	1.307	0.132	0.015
	cc-pVTZ	1.284	0.126	0.070	1.311	1.300	0.129	0.016
	6-311++g(3df,3pd)					1.272	0.127	0.017

		H_{IF}	V_{IF}	S_{IF}
		Ref 30		
DFT, FO	TZ2P	0.334	0.141	0.023

		V_{IF}	ΔE_v
		Ref 44	
GMH-KTA	6-31 g*	0.137	1.574
CASSCF(7,8)	6-31 g*	0.098	1.799
CASSCF(11,12)	6-31 g*	0.097	1.415
CAS-PT2(11,12)	6-31 g*	0.081	1.175

[a] Use of the latter ones is explicitly indicated. [b] All energy quantities are expressed in eV.

MS-PT2, and tend to overcome these shortcomings. While, as discussed in ref 34, the comparison between the results from BHH and multireference calculations does not allow one to draw definitive conclusions in favor of either approach, my current results using eq 11 and the M06-HF functional clearly support the post-HF data. Furthermore, the results in Table 1 confirm the conclusions in ref 75 about the ability of this hybrid XC functional to correct for the unphysical electron self-interaction[63] and its considerable improvement on HF. In the M06-HF approximation,[73] the XC energy is obtained by adding the nonlocal HF exchange energy, as computed from the occupied Kohn−Sham orbitals, to XC energy with the same local functional form as for M06-L but different values of the parameters that enforce its compatibility with the presence of full HF exchange. Ultimately, M06-HF includes both local and nonlocal exchange, but only the latter survives at large enough distances, thereby providing the correct asymptotic behavior. Moreover, it satisfies the uniform-electron-gas limit at both the short and long range, which is an important formal property, and includes short-range static-correlation effects that are missing in hybrid functionals where the HF exchange is added to pure correlation energy. Such features can also lead, on the average, to a better description of the ground-state energetics than that given by the popular B3LYP functional.[73] By considering the ingredients in eq 11, the optimal performance of the M06-HF functional might be attributed to an equilibrated description of the ground state, with a good medium−long-range behavior of the exchange in the considered GT system. This avoids an excessive spread of the valence charge over the two nucleobases, which would otherwise amount to exceedingly similar values of a and b in eqs 11 and a correspondingly overestimated transfer integral. The investigation of other DNA nucleobase stacks is however necessary to confirm this indication and is the subject of future work, also considering the low computational cost of the hybrid-DFT implementation of eq 11. In this regard, it is noteworthy that the M06-HF functional shows an optimal performance even at the 6-31g* level of computation, which is an important point for first-principles calculations of charge-transfer integrals on large-scale systems.

Note that in eq 11 the DFT energies appear only in ΔE_{IF}, that is, the difference between the energies of the whole system in the two diabatic states for the given nuclear coordinates. Hence, the addition of the dispersion terms according to the recipes allowed by the employed computational chemistry package[81] does not

Table 2. Quality of the Two-State Approximation Using TP and CDFT Diabatic States, Quantified in the First Two Data Columns via the Square Modulus of the Ground-State Wave Function That Results from the First Expansion in eq 2, and the Overlap Integrals of the Diabatic States Belonging to the TP and CDFT Sets (C_{ij}) Obtained from eqs 36a and 36b, by Inserting the Values of S_{IF} and $\overline{S}_{IF}$ from the Calculations (First Line for Each Functional) or Directly from the Computed Wave Functions (Second Line)

		$\langle\psi\|\psi\rangle_{CDFT}$	$\langle\psi\|\psi\rangle_{TP}$	C_{11}	C_{22}	C_{12}	C_{21}	$(C_{12}+C_{21})/2$
M06-2x	eqs 36a and 36b			0.9995	0.9995	0.0499	0.0499	0.0499
	computation	0.9983	0.9917	0.9930	0.9910	0.0508	0.0488	0.0498
M06-HF	eqs 36a and 36b			0.9997	0.9997	0.0404	0.0404	0.0404
	computation	0.9995	0.9934	0.9940	0.9910	0.0395	0.0410	0.0403

change the value of the charge-transfer integral resulting from eq 11. Furthermore, as discussed elsewhere,[48] the approach is also robust against the basis set superposition error (BSSE). In this work, it is shown by the data at the M06-2x/cc-pVTZ and M06-HF/cc-pVTZ computational levels in Table 1, which were obtained using the counterpoise method.[83]

The cc-pVTZ basis set[84] was used to compute V_{IF} with both the TP and CDFT diabatic states. The two diabatic sets lead to very similar V_{IF} values against significantly different overlaps S_{IF} in either M06-2X or M06-HF calculations. Indeed, the differences in the transfer integral values can be essentially ascribed to the slight overestimation of ΔE_{IF} by eq 35. The similarity of the V_{IF} values, the fulfillment of the two-state approximation regarding the values of[85] $\langle\psi|\psi\rangle = a^2 + b^2 + 2abS_{IF}$ (Table 2), and the nature of the system, where the D and A groups are spatially well separated, support the use of both TP and CDFT states, which are then expected to satisfy eqs 16 and 17. To see this, the quantities (obtained from eq 16)

$$C_{11} \equiv \langle\psi_I|\overline{\psi}_I\rangle = C_{22} \equiv \langle\psi_F|\overline{\psi}_F\rangle = \frac{1}{2}\left[\sqrt{\frac{1+\overline{S}_{IF}}{1+S_{IF}}} + \sqrt{\frac{1-\overline{S}_{IF}}{1-S_{IF}}} + \left(\sqrt{\frac{1+\overline{S}_{IF}}{1+S_{IF}}} - \sqrt{\frac{1-\overline{S}_{IF}}{1-S_{IF}}}\right)S_{IF}\right] \quad (36a)$$

$$C_{12} \equiv \langle\psi_I|\overline{\psi}_F\rangle = C_{21} \equiv \langle\psi_F|\overline{\psi}_I\rangle = \frac{1}{2}\left[\sqrt{\frac{1+\overline{S}_{IF}}{1+S_{IF}}} - \sqrt{\frac{1-\overline{S}_{IF}}{1-S_{IF}}} + \left(\sqrt{\frac{1+\overline{S}_{IF}}{1+S_{IF}}} + \sqrt{\frac{1-\overline{S}_{IF}}{1-S_{IF}}}\right)S_{IF}\right] \quad (36b)$$

are considered. The overlaps between the CDFT and TP diabatic wave functions (identified with $\mathbf{\Psi}$ and $\overline{\mathbf{\Psi}}$, respectively) obtained from the M06-2x and M06-HF calculations are compared in Table 2 with the values obtained by insertion of S_{IF} and $\overline{S}_{IF}$ (see Table 1) into eqs 36a and 36b. The agreement is good, thus confirming the expectation. Notice that, although the $\overline{S}_{IF}$ values are smaller than the S_{IF} ones, and much smaller than unity, eq 11 (or its approximation in eq 10) must be used to obtain V_{IF} from nonorthogonal diabatic states. The corresponding value of H_{IF} can be obtained from eq 6 and is generally very different from V_{IF}, even if the involved energy quantities are computed in a one-orbital picture, as in ref 30 (see the H_{IF} and V_{IF} values reported in Table 1).

The assessment of the V_{IF} value for the hole transfer through the GT stack around 0.08 eV by both the CAS-PT2 method in ref 44 and the hybrid-DFT one at the M06-HF level in this work is in my opinion a useful step toward a systematic and consistent quantification of hole-transfer integrals between stacked nucleobases. This consistency needs to be assessed at a more extended level in future works, including calculations with the complementary nucleobases for the GT stack and on other DNA stacks. It is worth noticing that in the Marcus nonadiabatic regime, where the CT rate has a quadratic dependence on V_{IF},[17] a transfer integral of ∼0.08 eV rather than ∼0.13 eV amounts to a difference by a factor of ∼2.64 in the estimate of the CT rate, which brings about an important difference if hopping transport through a strand is considered. Anyway, if either hopping of localized charges[86,87] or polaron diffusive motion[88,89] is the effective transport mechanism, the charge transfer integral between neighboring units plays an important role in the electrical conduction through DNA systems.[90]

It is worth noting that all hybrid-DFT implementations lead to values of the vertical excitation energy between the CASSCF(11,12) and CAS-PT2(11,12) values, closer to the latter. In particular, while M06-2X appears to overestimate V_{IF}, it provides ΔE_v values that are located between the M06-HF and BHH ones. Indeed, a recent study[91] shows that M06-2X performs better than M06-HF, and widely used hybrid XC functionals such as B3LYP and PBE0, for the description of other types of excitations, i.e., vertical singlet excitations of adenine−thymine and guanine−cytosine base stacks. On the other hand, the M06-HF functional was designed[73] for accurate predictions of long-range CT excited states. Future studies with the most recent Minnesota hybrid meta density functionals (i.e., M08-HX and M08-SO,[92] which may be considered as improved versions of M06-2X,[93] also with reference to the self-interaction term in the correlation functional[92]) are desirable on the basis of the above results and discussion.

4.2. Hole and Electron Transfer Integrals in the Perylene-diimide Dimer. The hole and electron transfer integrals are calculated for the PDI-H (or simply PDI) dimer, with a hydrogen atom at the imide position. The geometry of the monomer was drawn from the Supporting Information of ref 14, and the dimer was built with the same shift parameters used in ref 14 for the CH_3 derivative. In particular, the stacking distance was fixed at 3.4 Å.[94] In order to move the dimer slightly away from the transition state coordinate Q_t, the H atoms in one of the monomers were further relaxed. The resulting geometry of the dimer corresponds to a value Q of the reaction coordinate very close to Q_t ($Q = Q_t + \delta Q$), as quantified by the fact that $\Delta E_{IF}(Q) \ll 2V_{IF}(Q)$ (see Table 3 and also Table S1 in the Supporting Information).

Considering that the PDI molecule is a kind of cyclic polyene, the M06-2X functional was first used in the calculations, thereby following the indications that result from ref 75 and the excellent performance achieved in ref 14. The hole-transfer ($V_{IF}^{(h)}$) and electron-transfer ($V_{IF}^{(e)}$) integrals obtained using the 6-311g** basis set are reported in the first row of Table 3 (values of the

Table 3. Hole ($V_{IF}^{(h)}$) and Electron ($V_{IF}^{(e)}$) Transfer Integrals and Corresponding Diabatic Energy Differences ($\Delta E_{IF}^{(h)}$ and $\Delta E_{IF}^{(e)}$) in the PDI Dimer, Using CDFT Diabatic Electronic States[a]

XC functional	basis set	$V_{IF}^{(h)}$	$\Delta E_{IF}^{(h)}$	$V_{IF}^{(e)}$	$\Delta E_{IF}^{(e)}$
M06-2x	6-311 g**	35.2−35.9	0.04−0.40	127.6−129.7	0.10−0.95
	6-311 g**/6-311++g*	41.5		138.2	
BHH	6-311 g**/6-311++g*			112.9	

[a] First row: ranges of values corresponding to different geometries (see main text) and using the M06-2X hybrid functional. Second and third rows: values at the nuclear coordinates $Q_t + \delta Q$, using the M06-2X and BHH XC functionals, respectively, with the mixed 6-311g**/6-311+g* basis set. All quantities are expressed in meV.

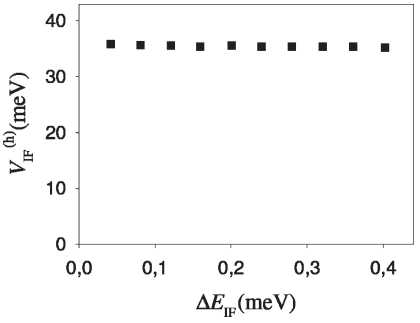

Figure 3. Effective electronic coupling for hole transfer in a PDI-H stack (*x* shift =1.60 Å, *y* shift =0.94 Å, *z* shift = 3.40 Å). The *y* axis starts from 0 meV to point up the small relative spread of the data points.

effective electronic coupling and the diabatic energy difference at the left and right sides, respectively, of each reported interval). They are close to the effective couplings for the CH_3 derivative provided in ref 14.

By assuming the Condon approximation in $[Q_t, Q_t + \delta Q]$, the computational accuracy allowed by eq 11 near Q_t was tested by calculating $V_{IF}^{(h)}$ also at the atomic positions $Q_j = Q_t + j\delta Q/10$, with j = 1 to 9. A further test was performed on $V_{IF}^{(e)}$, at nuclear coordinates $Q_j = Q_t + j\delta Q/10$, with j = 1 and 5. The ranges of values in the first line of Table 3 were thus obtained (see individual values in Table S1 of the Supporting Information). Such narrow ranges, with a maximum difference of less than 2%, show the high accuracy of the transfer integral calculation using eq 11, irrespective of the fact that the differences in the values may actually be ascribed to computational uncertainty or small deviation from the Condon approximation. The small spread in the $V_{IF}^{(h)}$ values is also displayed in Figure 3. ΔE_{IF}[95] is chosen as the reaction coordinate, which highlights the proximity to Q_t (cf. the energy ranges on the two axes).

The values of $V_{IF}^{(h)}$ and $V_{IF}^{(e)}$ were also calculated by using a composite 6-311g**/6-311+g* basis set. To obtain a proper spanning of the intermolecular space, despite the limited amount of diffuse functions allowed by the available CDFT implementation, the basis set was augmented on O and N atoms, and the C atoms mainly involved in the spatial distributions of the frontier orbitals according to the calculations at the M06-2X/6-311g** level. The $V_{IF}^{(h)}$ and $V_{IF}^{(e)}$ values remain close to those for the CH_3 derivative in ref 14. In particular, the large value of the electron-transfer integral is confirmed.

The calculation at the BHH/6-311g**/6-311+g* level confirms the high value of $V_{IF}^{(e)}$. Hence, the PDI system, without a specific substituent at the imide position, is also a promising candidate for incorporation into electronic devices where excess electron transport is exploited. BHH yields a value of $V_{IF}^{(e)}$ that is about 20% smaller than that provided by M06-2X. Indeed, any XC density functional is an approximation of the unknown exact one and can be affected by spurious electron self-interaction,[63] with consequent errors in electronic coupling valuations. Thus, the difference in the BHH and M06-2X values of $V_{IF}^{(e)}$ is the result of different approximations to the exact XC functional, and both values can be, in principle, affected by errors. However, for the same reason that BHH and M06-2X are quite different approximations, the two values contribute to identify a probable range for the value of $V_{IF}^{(e)}$, whence comes the order of magnitude of its uncertainty. This is valuable information, all the more so that the size of the system is prohibitive for multireference calculations.

The above comparison and the consistency of the M06-2X values near Q_t denote good performance of the M06-2X hybrid XC functional for the PDI system. This is an important point in favor of M06-2X compared to many other XC functionals, which for large and complicated electronic systems often suffer from fundamental problems that may lead to divergence or convergence to an energy saddle point rather than to the ground-state minimum.[96] Indeed, the considered PDI system at the given nuclear coordinates offers a paradigmatic case in this respect. In fact, the calculations of $V_{IF}^{(h)}$ using BHH and of $V_{IF}^{(e)}$ using both BHH and M06-HF showed problematic convergence and led to broken-symmetry charge-localized solutions for the ground-state wave function, which did not allow suitable computation of $V_{IF}^{(h)}$ and $V_{IF}^{(e)}$.

4.3. Long-Range Electron Transfer in the Quinol-Semiquinone Redox Couple. Following refs 73 and 75, the M06-HF density functional was used to study the dependence of the charge-transfer integral on the distance between donor and acceptor. Similarly to recent results,[37] the transfer integral values in a semilog plot lie approximately on a straight line (see black data points and best-fit line in Figure 4); thus

$$V_{IF} \cong V_0 \exp(-\beta R_{\mathscr{D}\mathscr{A}}) \qquad (37)$$

where V_0 is a suitable constant, $R_{\mathscr{D}\mathscr{A}}$ is the donor−acceptor distance, and β is the decay factor. On the basis of the whole set of data points, the decay factor is β = 2.07 Å^{-1}, which is larger than the value of 1.7 Å^{-1} predicted by the pathway model.[97] However, if the fit is performed for $\mathscr{D}-\mathscr{A}$ separations between 3 and 6 Å, where eq 37 turns out to be well-satisfied, a decay factor β = 1.64 Å^{-1} is obtained (gray line). On the other hand, eq 34 turns out to be valid at large enough $\mathscr{D}-\mathscr{A}$ distances ($R_{\mathscr{D}\mathscr{A}} \geq$ 3.5 Å in the graph of Figure 4). In particular, the red squares are computed using the first approximate equality in eq 34.

The results in Figure 4 support the use of the full-HF-exchange M06-HF hybrid functional over a large range of $\mathscr{D}-\mathscr{A}$ separations. Indeed, for the face-to-face quinol−semiquinone system, the implementation of eq 11 using CDFT diabatic states and the M06-HF functional appears to perform reasonably well even at

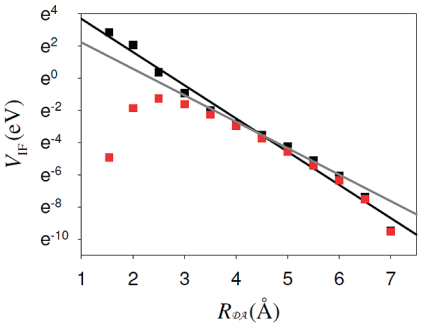

Figure 4. Electron transfer integral (on a natural logarithm scale) vs the donor−acceptor distance $R_{\mathscr{D}\mathscr{A}}$, obtained using eq 11 (black) and the first equality in eq 34 (red), which clearly fails at small distances. A mixed cc-pVTZ/aug-cc-pVTZ basis set is used, with diffuse functions added on the O atoms for a proper spanning of the intermolecular space. The black and gray best-fit lines are described in the main text.

the shortest explored distance $R_{\mathscr{D}\mathscr{A}}$ = 1.54 Å, where the overlap integral is unduly large, S_{IF} = 0.949 (Table S2 in the Supporting Information), so that the definition of the CDFT states reaches the largest uncertainty.[32] Yet, the value of V_{IF} is 17.2 eV and differs by about 2% from the value of 17.6 eV in ref 37. Clearly, both values can, in principle, be wrong. However, they are obtained from different theoretical-computational setups (except for the common use of CDFT diabatic states), and hence the similarity of the results gives support to their reliability. The results in this section also support the use of CDFT diabatic states in short-range and/or intramolecular CT, but in the latter case, the donor and acceptor groups are not separated, so it is important to check that any reliable electron density constraint, which includes the atoms of a redox site dictated by suitable chemical reasons, leads to the same value of the effective electronic coupling.

5. CONCLUDING REMARKS

I recently proposed[34] a formula (i.e., eq 11 in this paper) for the calculation of charge-transfer integrals using a few electronic quantities that characterize the diabatic states and that can be easily obtained from *ab initio* computation. Equation 11 applies to both orthogonal and nonorthogonal diabatic states and is exact within the two-state model. This is useful in all of those cases where the nature of the CT system suggests the use of a nonorthogonal diabatic representation. Moreover, the results of this work markedly indicate that the quantities involved in eq 11 can be obtained from CDFT[32] diabatic states, even if such states are characterized by a relatively large overlap (or a large one, e.g., for the quinol−semiquinone redox system at short distance). This is to be considered also in future studies of short-range intramolecular CT reactions.

From an exquisitely theoretical point of view, this work (i) relates eq 11 to previous approaches to V_{IF} calculation, (ii) establishes its connection with Löwdin's transformation, (iii) fully characterizes V_{IF}, as defined[8] in eq 6 (thereby, also as expressed by eq 11), as the effective electronic coupling or perturbation that is involved in the probability of transition between nonorthogonal electronic states, and (iv) establishes the relation between charge-transfer and overlap integrals in the long-range CT between off-resonance diabatic states, without the use of empirical parameters.

As shown in section 2.2, the application of eq 11 to nonorthogonal diabatic states is equivalent to the exact Löwdin transformation[40] of such states and use of the same eq 11 or eq 10 (for zero overlap) with the Löwdin orthogonal states. Anyhow, given a physically meaningful set of nonorthogonal diabatic states, eq 11 can be directly used by calculating the necessary quantities on these states without a need for their prior orthogonalization or any approximation based on the magnitude of the overlap.

On the one hand, the analysis in section 2.2 and the Appendix clarifies the relation between eq 11 and other methods in the previous literature[22,27,41,42] that use orthogonal diabatic electronic states and where the latter can be obtained from rotation of the adiabatic states.[27] In particular, it is observed that, once an appropriate nonorthogonal diabatic representation of the CT reaction under consideration is known, the correct rotation of the adiabatic states must lead to orthogonal diabats related to the nonorthogonal ones by the Löwdin transformation. Thus, any criterion for obtaining the diabatic states directly by rotation of the adiabatic ones should be confronted with indications resulting form the nature of the CT system and the way it is initially prepared (e.g., depending on the initial localization of the charge in a redox moiety and the distance between donor and acceptor, hence the spread of the initial electron charge distribution on a near redox site). In this respect, in my opinion, the CDFT approach affords a "natural" localization of the transferring electron charge, since it searches for the charge distribution of minimum energy under the constraint of charge localization around a given set of atoms which can be inferred and thus selected on the basis of chemical grounds. Then, eq 11 allows the use of the CDFT diabatic states without approximations, within the two-state model.

On the other hand, since eq 11 is obtained by direct solution of the two-state secular equation by using the definition of V_{IF} in eq 6, working with nonorthogonal states requires that eq 6 indeed provides the effective coupling in the nonorthogonal representation of a two-state dynamical problem. This is not a trivial point considering that the effective Hamiltonian is represented by a non-Hermitian matrix (see eq 25b), whereas V_{IF} from eq 6 is the off-diagonal element of a Hermitian operator. In order to extricate this delicate conceptual problem, eq 29 of this paper shows that V_{IF} from eq 6 gives, as desired, the effective perturbation involved in the transition between two nonorthogonal electronic states at any fixed nuclear coordinates. Equation 29 can be considered as an appropriate extension of Rabi's formula to the case of nonorthogonal electronic states. In particular, similarly to the latter, it gives the maximum oscillation of the transition probability for isoenergetic initial and final electronic states. Ultimately, although the effective Hamiltonian for the two-state model using nonorthogonal diabatic states is, in general, represented by a non-Hermitian operator and various devices have been used to regain the desired Hermitian behavior,[15] eqs 26 and 29 yield the role of the perturbation term in the Hermitian component of the Hamiltonian. Therefore, with reference to CT processes, eq 6, hence its expression in eq 11, provides the appropriate expression of the effective coupling between nonorthogonal states, and not just an *ad hoc* symmetrized expression of such coupling.

The computational results of this work contribute to delimiting the theoretical expectation values of the effective electronic coupling for the considered CT reactions and support selective use of the Minnesota hybrid meta density functionals[75] for the study of diverse kinds of CT systems. However, in general, the results of this work, in agreement with previous ones,[34,48] stress the importance of using different hybrid XC functionals and basis

sets as a crucial rule in order to identify reliable DFT values or probable ranges of values for the charge-transfer integral in many redox systems.

The BHH functional performs better than the M06-2X one for the computation of the charge-transfer integral in the guanine−thymine stack, if the results from multireference calcualtions[44] reported in Table 1 are taken as reference values. On the contrary, M06-HF gives values of the charge-transfer integral and the vertical excitation energy very close to those from the multireference calculations.[44] This fosters use of this hybrid functional in other DNA stacks, and also further investigation into the presence of complete Watson−Crick pairs. Moreover, M06-HF is expected to be particularly useful for studying triplets of base pairs, where long-range CT is also involved. On the basis of the current and previous[34,48] results, M06-HF and BHH may provide the best set of hybrid functionals to be applied in the investigation of the hole transfer through nucleobase stacks. Nevertheless, it is worth noting that the M06-2X density functional shows optimal performance in the calculation of the vertical excitation energy for the GT stack.

Overall, M06-2X does much better than all other XC functionals tested on the perylenediimide stack. The analysis of this large π-electron system points to M06-2X as the most robust XC functional against convergence problems in the iterative solution of Kohn−Sham equations. It allowed the calculation of the hole and electron transfer integrals in the PDI stack very close to its transition state coordinate with high computational accuracy.

Finally, long-range CT has been studied in the quinol−semiquinone redox couple, for which M06-HF gives a V_{IF} decay factor in the expected range[37,97] and confirms the theoretical expectation of eq 34.

Ultimately, the computational results of this paper suggest BHH, M06-2X, and M06-HF as a good set of hybrid functionals for charge-transfer integral calculations in various molecular systems. Clearly, future investigation of the most recent M08-HX and M08-SO[92] Minnesota functionals is desirable.

APPENDIX

Wave Function Overlap Method and Löwdin Transformation. The row matrix $\overline{\mathbf{\Psi}} = (\bar{\psi}_I\ \bar{\psi}_F)$ is related to the orthogonal set $\boldsymbol{\chi} = (\chi_I\ \chi_F)$ by the equation

$$\boldsymbol{\chi} = \overline{\mathbf{\Psi}}\overline{\mathbf{S}}^{-1/2} \tag{38}$$

where

$$\overline{\mathbf{S}} = \begin{pmatrix} 1 & \overline{S}_{IF} \\ \overline{S}_{IF} & 1 \end{pmatrix} \tag{39}$$

By equating the right-hand sides of eqs 14 and 38, and multiplying on the right by the matrix $\overline{\mathbf{S}}^{1/2}$, the following is obtained:

$$\overline{\mathbf{\Psi}} = \mathbf{\Psi}\mathbf{S}^{-1/2}\overline{\mathbf{S}}^{1/2} \tag{40}$$

The matrix $\mathbf{S}^{-1/2}$ is given by[60,98]

$$\mathbf{S}^{-1/2} = \frac{1}{2}\begin{pmatrix} 1/\sqrt{1+S_{IF}} + 1/\sqrt{1-S_{IF}} & 1/\sqrt{1+S_{IF}} - 1/\sqrt{1-S_{IF}} \\ 1/\sqrt{1+S_{IF}} - 1/\sqrt{1-S_{IF}} & 1/\sqrt{1+S_{IF}} + 1/\sqrt{1-S_{IF}} \end{pmatrix} \tag{41}$$

and

$$\overline{\mathbf{S}}^{1/2} = \frac{1}{2}\begin{pmatrix} \sqrt{1+\overline{S}_{IF}} + \sqrt{1-\overline{S}_{IF}} & \sqrt{1+\overline{S}_{IF}} - \sqrt{1-\overline{S}_{IF}} \\ \sqrt{1+\overline{S}_{IF}} - \sqrt{1-\overline{S}_{IF}} & \sqrt{1+\overline{S}_{IF}} + \sqrt{1-\overline{S}_{IF}} \end{pmatrix} \tag{42}$$

The insertion of eqs 41 and 42 into eq 40 gives eq 17. Moreover, the comparison of eqs 17 and 41 shows that $\mathbf{M} = \mathbf{S}^{-1/2}$ when $\overline{\mathbf{S}}$ is the identity matrix, i.e., when $\overline{S}_{IF} = 0$, which gives eq 14 as a special case of eq 16.

Finally, I wish to show how the insertion of eq 14 into eq 10 leads to eq 11. According to eqs 14 and 41, the energies of the orthogonal states χ_I and χ_F are related to those of the nonorthogonal ones ψ_I and ψ_F by

$$E(\chi_I) = (\mathbf{S}^{-1/2})_{11}^2 E(\psi_I) + (\mathbf{S}^{-1/2})_{12}^2 E(\psi_F) + 2(\mathbf{S}^{-1/2})_{11}(\mathbf{S}^{-1/2})_{12}\langle\psi_I|H|\psi_F\rangle \tag{43}$$

and

$$E(\chi_F) = (\mathbf{S}^{-1/2})_{12}^2 E(\psi_I) + (\mathbf{S}^{-1/2})_{11}^2 E(\psi_F) + 2(\mathbf{S}^{-1/2})_{11}(\mathbf{S}^{-1/2})_{12}\langle\psi_I|H|\psi_F\rangle \tag{44}$$

where the symmetry of $\mathbf{S}^{-1/2}$ has been exploited. Therefore, the corresponding diabatic energy differences $\Delta E_{IF}(\boldsymbol{\chi}) \equiv E(\chi_I) - E(\chi_F)$ and $\Delta E_{IF}(\mathbf{\Psi}) \equiv E(\psi_I) - E(\psi_F)$ satisfy the equation

$$\Delta E_{IF}(\boldsymbol{\chi}) = [(\mathbf{S}^{-1/2})_{11}^2 - (\mathbf{S}^{-1/2})_{12}^2]\Delta E_{IF}(\mathbf{\Psi}) = \frac{\Delta E_{IF}(\mathbf{\Psi})}{\sqrt{1-S_{IF}^2}} \tag{45}$$

Alternatively, this result can be obtained by equating the expressions of the vertical excitation energy for the two diabatic sets. The wave function overlaps are related by the equations

$$A(\chi) \equiv \langle\chi_I|\psi\rangle = (\mathbf{S}^{-1/2})_{11}A(\psi) + (\mathbf{S}^{-1/2})_{12}B(\psi) \tag{46}$$

and

$$B(\chi) \equiv \langle\chi_F|\psi\rangle = (\mathbf{S}^{-1/2})_{12}A(\psi) + (\mathbf{S}^{-1/2})_{11}B(\psi) \tag{47}$$

Then,

$$V_{IF} = \left|\frac{A(\boldsymbol{\chi})B(\boldsymbol{\chi})}{A^2(\boldsymbol{\chi}) - B^2(\boldsymbol{\chi})}\Delta E_{IF}(\boldsymbol{\chi})\right| = \left|\frac{[(\mathbf{S}^{-1/2})_{11}^2 + (\mathbf{S}^{-1/2})_{12}^2]A(\mathbf{\Psi})B(\mathbf{\Psi}) + (\mathbf{S}^{-1/2})_{11}(\mathbf{S}^{-1/2})_{12}[A^2(\mathbf{\Psi}) + B^2(\mathbf{\Psi})]}{[(\mathbf{S}^{-1/2})_{11}^2 - (\mathbf{S}^{-1/2})_{12}^2][A^2(\mathbf{\Psi}) - B^2(\mathbf{\Psi})]} \times \frac{\Delta E_{IF}(\mathbf{\Psi})}{\sqrt{1-S_{IF}^2}}\right| = \left|\frac{A(\mathbf{\Psi})B(\mathbf{\Psi})}{A^2(\mathbf{\Psi}) - B^2(\mathbf{\Psi})}\Delta E_{IF}(\mathbf{\Psi})\left[1 - \frac{A^2(\mathbf{\Psi}) + B^2(\mathbf{\Psi})}{2A(\mathbf{\Psi})B(\mathbf{\Psi})}S_{IF}\right]\frac{1}{1-S_{IF}^2}\right| \tag{48}$$

that is the expression in eq 11b.

ASSOCIATED CONTENT

Supporting Information. Table S1, which contains the values of the effective electronic couplings and diabatic energy differences in the PDI stack at the coordinates Q_j (j = 1 to 10), and Table S2, which includes the effective electronic couplings, diabatic energy differences, and overlaps for the quinol-semiquinone system

at the considered distances. This material is available free of charge via the Internet at http://pubs.acs.org.

AUTHOR INFORMATION

Corresponding Author

*Phone: +972-3-6407634. Fax: +972-3-6409293. E-mail: migliore@post.tau.ac.il.

ACKNOWLEDGMENT

I am thankful to Abraham Nitzan for his scientific and human support during the elaboration of this work. I thank Stefano Corni, Rosa Di Felice, and Joseph Subotnik for useful discussions. I acknowledge support of this research from the Israel Science Foundation and the European Science Council (FP7/ERC grant number 226628).

REFERENCES

(1) Slowinski, K.; Chamberlain, R. V.; Miller, C. J.; Majda, M. *J. Am. Chem. Soc.* **1997**, *119*, 11910–11919.
(2) Napper, A. M.; Liu, H.; Waldeck, D. H. *J. Phys. Chem. B* **2001**, *105*, 7699–7707.
(3) Chi, Q.; Zhang, J.; Jensen, P. S.; Christensen, H. E. M.; Ulstrup, J. *Faraday Discuss.* **2006**, *131*, 181–195.
(4) Sek, S.; Palys, B.; Bilewicz, R. *J. Phys. Chem. B* **2002**, *106*, 5907–5914.
(5) Jensen, P. S.; Chi, Q.; Zhang, J.; Ulstrup, J. *J. Phys. Chem. C* **2009**, *113*, 13993–14000.
(6) Chi, Q.; Zhang, J.; Arslan, T.; Borg, L.; Pedersen, G. W.; Christensen, H. E. M.; Nazmudtinov, R. R.; Ulstrup, J. *J. Phys. Chem. B* **2010**, *114*, 5617–5624.
(7) Feng, X.; Marcon, V.; Pisula, W.; Hansen, M. R.; Kirkpatrick, J.; Grozema, F.; Andrienko, D.; Kremer, K.; Müllen, K. *Nat. Mater.* **2009**, *8*, 421–426.
(8) Farazdel, A.; Dupuis, M.; Clementi, E.; Aviram, A. *J. Am. Chem. Soc.* **1990**, *112*, 4206–4214.
(9) Nitzan, A. *Annu. Rev. Phys. Chem.* **2001**, *52*, 681–750.
(10) Tong, G. S. M.; Kurnikov, I. V.; Beratan, D. N. *J. Phys. Chem. B* **2002**, *106*, 2381–2392.
(11) Rösch, N.; Voityuk, A. A. *Top. Curr. Chem.* **2004**, *237*, 37–72 and references therein.
(12) Corni, S. *J. Phys. Chem. B* **2005**, *109*, 3423–3430.
(13) Kuznetsov, A. M.; Medvedev, I. G.; Ulstrup, J. *J. Chem. Phys.* **2009**, *131*, 164703.
(14) Vura-Weis, J.; Ratner, M. A.; Wasielewski, M. R. *J. Am. Chem. Soc.* **2010**, *132*, 1738–1739.
(15) Newton, M. D. *Chem. Rev.* **1991**, *91*, 767–792 and references therein.
(16) Marcus, R. A. *J. Chem. Phys.* **1956**, *24*, 966–978. **1956**, 979–989.
(17) Marcus, R. A.; Sutin, N. *Biochim. Biophys. Acta* **1985**, *811*, 265–322.
(18) Kuznetsov, A. M.; Ulstrup, J. *Electron Transfer in Chemistry and Biology*; John Wiley & Sons: New York, 1999.
(19) (a) Landau, L. D. *Phys. Z. Sowjetunion* **1932**, *1*, 88. **1932**, *2*, 46. (b) Zener, C. . *Proc. R. Soc. London, Ser. A* **1932**, *137*, 696–702. **1933**, *140*, 660–668.
(20) Marcus, R. A. *Annu. Rev. Phys. Chem.* **1964**, *15*, 155–196.
(21) Zhang, L. Y.; Friesner, R. A.; Murphy, R. B. *J. Chem. Phys.* **1997**, *107*, 450–459.
(22) (a) Cave, R. J.; Newton, M. D. *Chem. Phys. Lett.* **1996**, *249*, 15–19.(b) *J. Chem. Phys.* **1997**, *106*, 9213−9226.
(23) Skourtis, S. S.; Beratan, D. N. *Adv. Chem. Phys.* **1999**, *106*, 377–452.
(24) Regan, J. J.; Onuchic, J. N. *Adv. Chem. Phys.* **1999**, *107*, 497–553.
(25) Prezhdo, O. V.; Kindt, J. T.; Tully, J. C. *J. Chem. Phys.* **1999**, *111*, 7818–7827.
(26) Voityuk, A.; Rösch, N.; Bixon, M.; Jortner, J. *J. Phys. Chem. B* **2000**, *104*, 9740–9745.
(27) Voityuk, A. A.; Rösch, N. *J. Chem. Phys.* **2002**, *117*, 5607–5616.
(28) Zheng, X. H.; Stuchebrukhov, A. A. *J. Phys. Chem. B* **2003**, *107*, 9579–9584.
(29) Bredas, J. L.; Beljonne, D.; Coropceanu, V.; Cornil, J. *Chem. Rev.* **2004**, *104*, 4971–5003.
(30) Senthilkumar, K.; Grozema, F. C.; Fonseca Guerra, C.; Bickelhaupt, F. M.; Lewis, F. D.; Berlin, Y. A.; Ratner, M. A.; Siebbeles, L. D. A. *J. Am. Chem. Soc.* **2005**, *127*, 14894–14903.
(31) Nishioka, H.; Kimura, A.; Yamato, T.; Kawatsu, T.; Kakitani, T. *J. Phys. Chem. B* **2005**, *109*, 1978–1987.
(32) (a) Wu, Q.; Van Voorhis, T. *Phys. Rev. A* **2005**, *72*, 024502.(b) *J. Chem. Phys.* **2006**, *125*, 164105.
(33) Migliore, A.; Corni, S.; Di Felice, R.; Molinari, E. *J. Chem. Phys.* **2006**, *124*, 064501.
(34) Migliore, A. *J. Chem. Phys.* **2009**, *131*, 114113.
(35) Glaesemann, K. R.; Govind, N.; Krishnamoorthy, S.; Kowalski, K. *J. Phys. Chem. A* **2010**, *114*, 8764–8771.
(36) Mikołajczyk, M. M.; Zaleśny, R.; Czyżnikowska, Ż.; Toman, P.; Leszczynski, J.; Bartkowiak, W. *J. Mol. Model.* [Online] DOI: 10.1007/s00894-010-0865-7.
(37) de la Lande, A.; Salahub, D. R. *THEOCHEM* **2010**, *943*, 115–120.
(38) Nowak, M. J.; Lapinski, L.; Kwiatkowski, J. S.; Leszczynski, J. *Computational Chemistry: Reviews of Current Trends*; Leszczynski, J., Ed.; World Scientific: Singapore, 1997; Vol. 2, pp 140−216.
(39) Cremer, D. *Mol. Phys.* **2001**, *99*, 1899–1940.
(40) Löwdin, P. O. *J. Chem. Phys.* **1950**, *18*, 365–375.
(41) Sanz, J. F.; Malrieu, J.-P. *J. Phys. Chem.* **1993**, *97*, 99–106.
(42) Creutz, C.; Newton, M. D.; Sutin, N. *J. Photochem. Photobiol. A: Chem.* **1994**, *82*, 47–59.
(43) Numrich, R. W.; Truhlar, D. G. *J. Phys. Chem.* **1975**, *79*, 2745–2766.
(44) Blancafort, L.; Voityuk, A. A. *J. Phys. Chem. A* **2006**, *110*, 6426–6432.
(45) Nakamura, H.; Truhlar, D. G. *J. Chem. Phys.* **2001**, *115*, 10353–10372.
(46) (a) Franck, J.; Dymond, E. G. *Trans. Faraday Soc.* **1926**, *21*, 536−542. (b) Condon, E. U. *Phys. Rev.* **1926**, *28*, 1182–1201.
(47) Weissbluth, M. *Atoms and Molecules*; Academic Press: New York, 1978; p 587.
(48) Migliore, A.; Corni, S.; Varsano, D.; Klein, M. L.; Di Felice, R. *J. Phys. Chem. B* **2009**, *113*, 9402–9415.
(49) A careful discussion of the relations among the crossing of the diabatic energy surfaces, the transfer integral, and the minimum adiabatic energy splitting when other electronic states are involved, and thus an effective two-state model is usually employed, can be found in ref 15.
(50) (a) Mulliken, R. S. *J. Am. Chem. Soc.* **1952**, *74*, 811–824. (b) Hush, N. S. *Prog. Inorg. Chem.* **1967**, *8*, 391–444. (c) Hush, N. S. *Electrochim. Acta* **1968**, *13*, 1005–1023. (d) Reimers, J. R.; Hush, N. S. *J. Phys. Chem.* **1991**, *95*, 9773–9781.
(51) Mulliken, R. S.; Person, W. B. *Molecular Complexes*; Wiley: New York, 1969.
(52) Valero, R; Song, L.; Gao, J.; Truhlar, D. G. *J. Chem. Theory Comput.* **2009**, *5*, 1–22.
(53) Kubař, T.; Woiczikowski, P. B.; Cuniberti, G.; Elstner, M. *J. Phys. Chem. B* **2008**, *112*, 7937–7947.
(54) Migliore, A.; Corni, S.; Di Felice, R.; Molinari, E. *J. Phys. Chem. B* **2006**, *110*, 23796–23800.
(55) Migliore, A.; Corni, S.; Di Felice, R.; Molinari, E. *J. Phys. Chem. B* **2007**, *111*, 3774.
(56) Migliore, A.; Sit, P. H.-L.; Klein, M. L. *J. Chem. Theory Comput.* **2009**, *5*, 307–323.
(57) Wolfsberg, M.; Helmholtz, L. *J. Chem. Phys.* **1952**, *20*, 837–843.
(58) Stuchebrukhov, A. A. *J. Chem. Phys.* **2003**, *118*, 7898–7906.
(59) Song, L.; Gao, J. *J. Phys. Chem. A* **2008**, *112*, 12925–12935.
(60) Rossi, M.; Sohlberg, K. *J. Phys. Chem. C* **2009**, *113*, 6821–6831.
(61) Sit, P. H.-L.; Cococcioni, M.; Marzari, N. *Phys. Rev. Lett.* **2006**, *97*, 028303.

(62) The electron wave functions considered in ref 40 are, indeed, atomic orbitals. Full-electron states are used in the present discussion in harmony with the computation methods employed in this paper.
(63) Koch, W.; Holthausen, M. C. *A Chemist's Guide to Density Functional Theory*; Wiley: New York, 2000; pp 53−54 (spin contamination), Chapters 2 and 6 (self-interaction).
(64) Note that the overlap matrix **S** defined in this paper, as well as in ref 58, corresponds to the sum of **S** and the identity matrix in ref 40.
(65) Dogonadze, R. R.; Urushadze, Z. D. *J. Electroanal. Chem.* **1971**, *32*, 235–245.
(66) Efrima, S.; Bixon, M. *J. Chem. Phys.* **1976**, *64*, 3639–3647.
(67) Bixon, M.; Jortner, J. *Adv. Chem. Phys.* **1999**, *106*, 35–202and references therein.
(68) Cave, R. J.; Baxter, D. V.; Goddard, W. A., III; Baldeschwieler, J. D. *J. Chem. Phys.* **1987**, *87*, 926–935 proposes an effective electronic coupling of the form $[(H_{IF} - H_{II}S_{IF})(H_{IF} - H_{FF}S_{IF})]^{1/2}/(1 - S_{IF}^2)$ where symmetry is achieved by means of geometric average. Also, other devices have been employed, as discussed in ref 15.
(69) Real wave functions are assumed here for the sake of simplicity, so that $S_{FI} = S_{IF}$ and $H_{FI} = H_{IF}$, as in eqs 3−6 and section 2.4. The relevant conclusions are not affected by this choice.
(70) Mulliken, R. S. *J. Phys. Chem.* **1952**, *56*, 295–311.
(71) Troisi, A.; Orlandi, G. *J. Phys. Chem. B* **2002**, *106*, 2093–2101.
(72) Becke, A. D. *J. Chem. Phys.* **1993**, *98*, 1372–1377.
(73) Zhao, Y.; Truhlar, D. G. *J. Phys. Chem. A* **2006**, *110*, 13126–13130.
(74) Zhao, Y.; Truhlar, D. G. *J. Chem. Phys.* **2006**, *125*, 194101.
(75) Zhao, Y.; Truhlar, D. G. *Theor. Chem. Acc.* **2008**, *120*, 215–241 and references therein.
(76) van der Boom, T.; Hayes, R. T.; Zhao, Y.; Bushard, P. J.; Weiss, E. A.; Wasielewski, M. R. *J. Am. Chem. Soc.* **2002**, *124*, 9582–9590.
(77) Bao, Z.; Locklin, J. J. *Organic Field-Effect Transistors*; CRC Press: Boca Raton, FL, 2007.
(78) Forquer, I.; Covian, R.; Bowman, M. K.; Trumpower, B. L.; Kramer, D. M. *J. Biol. Chem.* **2006**, *281*, 38459–38465.
(79) Grimaldi, S.; Arias-Cartin, R.; Lanciano, P.; Lyubenova, S.; Endeward, B.; Prisner, T. F.; Magalon, A.; Guigliarelli, B. *J. Biol. Chem.* **2010**, *285*, 179–187.
(80) Stowasser, R.; Hoffmann, R. *J. Am. Chem. Soc.* **1999**, *121*, 3414–3420.
(81) (a) Straatsma, T. P.; Aprà, E.; Windus, T. L.; Bylaska, E. J.; de Jong, W.; Hirata, S.; Valiev, M.; Hackler, M.; Pollack, L.; Harrison, R. *NWChem, A Computational Chemistry Package for Parallel Computers*, Version 5.1.1; Pacific Northwest National Laboratory: Richland, WA, 2008. (b) Kendall, R. A.; Apra, E.; Bernholdt, D. E.; Bylaska, E. J.; Dupuis, M.; Fann, G. I.; Harrison, R. J.; Ju, J.; Nichols, J. A.; Nieplocha, J.; Straatsma, T. P.; Windus, T. L.; Wong, A. T. *Comput. Phys. Commun.* **2000**, *128*, 260–283.
(82) Koopmans, T. *Physica* **1934**, *1*, 104.
(83) van Duijneveldt, F. B.; van Duijneveldt-van de Rijdt, J. G. C. M.; van Lenthe, J. H. *Chem. Rev.* **1994**, *94*, 1873–1885.
(84) Dunning, T. H., Jr. *J. Chem. Phys.* **1989**, *90*, 1007–1023.
(85) Normalized diabatic states and real *a* and *b* coefficients are obtained from the computation.
(86) Giese, B.; Amaudrut, J.; Köhler, A.-K.; Spormann, M.; Wessely, S. *Nature* **2001**, *412*, 318–320.
(87) Bixon, M.; Jortner, J. *J. Am. Chem. Soc.* **2001**, *123*, 12556–12567.
(88) Liu, C.-S.; Hernandez, R.; Schuster, G. B. *J. Am. Chem. Soc.* **2004**, *126*, 2877–2884.
(89) Conwell, E. M.; Bloch, S. M.; Mclaughlin, P. M.; Basko, D. M. *J. Am. Chem. Soc.* **2007**, *129*, 9175–9181.
(90) Grozema, F. C.; Tonzani, S.; Berlin, Y. A.; Schatz, G. C.; Siebbeles, L. D. A.; Ratner, M. A. *J. Am. Chem. Soc.* **2008**, *130*, 5157–5166.
(91) Aquino, A. J. A.; Nachtigallova, D.; Hobza, P.; Truhlar, D. G.; Hättig, C.; Lischka, H. *J. Comput. Chem.* **32, 2011**, 1217–1227.
(92) Zhao, Y.; Truhlar, D. G. *J. Chem. Theory Comput.* **2008**, *4*, 1849–1868.
(93) Zhao, Y.; Truhlar, D. G. *Chem. Phys. Lett.* **2011**, *502*, 1–13.
(94) Liu, S.-G.; Sui, G.; Cormier, R. A.; Leblanc, R. M.; Gregg, B. A. *J. Phys. Chem. B* **2002**, *106*, 1307–1315.
(95) Warshel, A. *J. Phys. Chem.* **1982**, *86*, 2218–2224.
(96) Høst, S.; Jansík, B.; Olsen, J.; Jørgensen, P.; Reine, S.; Helgaker, T. *Phys. Chem. Chem. Phys.* **2008**, *10*, 5344–5348.
(97) Jones, M. L.; Kurnikov, I. V.; Beratan, D. N. *J. Phys. Chem. A* **2002**, *106*, 2002–2006.
(98) Mayer, I. *Simple Theorems, Proofs, and Derivations in Quantum Chemistry*; Kluwer Academic/Plenum Publishers: New York, 2003; p 60.